

A simple model of current-voltage characteristic for surrounding gate short-channel nanowire MOSFET

STANKO M. OSTOJIĆ*, RAJKO M. ŠAŠIĆ

University of Belgrade, Faculty of Technology and Metallurgy, Karnegijeva 4, 11120 Belgrade, Serbia

A simple model of surrounding gate short-channel nanowire MOSFET current-voltage characteristic has been proposed. This model belongs to the class of drift-diffusion ones; it has been inspired by the corresponding long-channel models and should be considered as their naturally constructed extension. The accuracy of the developed model has been verified by comparison with available simulation results as well as with previous models calculations.

(Received October 29, 2015; accepted February 10, 2016)

Keywords: Surrounding Gate, Nanowire MOSFET, Short-Channel, 2D Analysis

1. Introduction

In the last fifteen years different types of multiple-gate MOSFETs with specific geometry tend to take place of planar MOSFETs and that way continue the dominance of unipolar devices in the traditional field of their application. Among them, cylindrical surrounding gate MOSFETs are believed to have the best control of short-channel effects. Therefore, the construction of reliable current-voltage characteristic for such devices including various procedures of Poisson's equation solving emerges as a huge challenge for a plenty of scientists. In the recent history of such efforts the model for long-channel devices based on the solution of one-dimensional (1D) Poisson's equation has been developed. This model included the nonzero doping concentration, while the extension of this model has examined the effect of carriers' mobility degradation [1]. But if we wish to continue beyond the conventional scaling limit two-dimensional analysis of Poisson's equation becomes necessary. The exact two-dimensional treatment is possible to be performed, but its results turn out not transparent enough and are not convenient for constructing models useful for practical purposes. That's why so much attention is paid to approximate analytical (as long as possible) solutions to the Poisson's equation. In the recent literature its two-dimensional solution is reported only in the case when the channel was fully depleted, i.e. in the case when the carriers concentration contribution to the Poisson's equation was totally ignored [2]. This procedure can only describe subthreshold regime, but fails in attempt to predict current-voltage characteristic above threshold [3].

The aim of this paper is not to ignore the described carriers' concentration contribution, i.e. to investigate the situation above threshold. The nonzero doping concentration has been maintained, while the carriers' mobility was set constant over the whole cross-section for the sake of simplicity (and independent on radial electric

field as well). The obtained results offer some interesting features.

2. Model description

Fig. 1 shows the cross-sectional view of cylindrical gate nanowire MOSFET considered in this paper. The source and drain are n^+ heavily doped, while the cylindrical silicon body is p-doped (N_A). R denotes silicon body radius, N_A -its doping concentration and t_{ox} being oxide thickness. There are no oxide charges, no work function difference exists and the flat band-voltage is set to be zero. For silicon body radius and doping concentration concerned in this paper the inversion layer quantum effects are verified to be negligible.

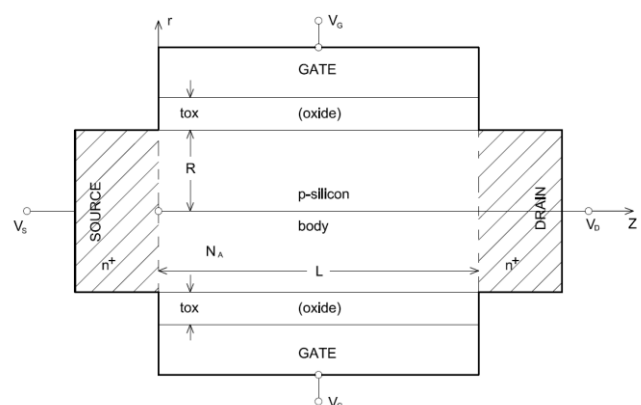


Fig. 1. A cross-sectional view of cylindrical gate nanowire MOSFET

Starting point of the suggested analysis is two-dimensional (2D) Poisson's equation written in cylindrical coordinates (the symmetry with respect to angular coordinate ϕ is already accounted for):

$$\frac{\partial^2 \psi}{\partial r^2} + \frac{1}{r} \frac{\partial \psi}{\partial r} + \frac{\partial^2 \psi}{\partial z^2} = \frac{q}{\epsilon_{Si}} N_A + \frac{q}{\epsilon_{Si}} n(r, z) \quad (1a)$$

$$n(r, z) = n_i \exp \frac{\psi - \psi_F}{\phi_t} \quad (1b)$$

valid for mobile charges concentration, where q is the electronic charge, n_i is the intrinsic silicon electron concentration, ϵ_{Si} is the permittivity of silicon $\phi_t = kT/q$ is the thermal potential and ψ_F is the quasi-Fermi level. Opposite to the subthreshold region, both fixed and mobile charge densities are not negligible. The one dimensional solution to this problem describing long-channel devices simply neglected the longitudinal term $\partial^2 \psi / \partial z^2$ in equation (1a) expecting it to be reasonably small due to the huge value of L/R ratio. But in the analysis intended to be performed in this paper, the mentioned ratio is considerably reduced. The question that naturally arises is how to take into account this longitudinal term with the tolerable level of simplicity loss. The first idea how to successfully achieve this goal is to set it constant, i.e. independent of coordinates r, z . This will not result in accurate solution of equation (1a) all over the examined structure, but undoubtedly is a step toward a satisfactory picture of mobile charge distribution in it. This constant should of course depend on drain-to-source voltage V_{DS} as a parameter, so the next step would be to make an educated guess and argue how should it look like. For small values of the parameter V_{DS} , the longitudinal term $\partial^2 \psi / \partial z^2$ should be proportional to it (V_{DS}) and L^{-2} (in the natural extension to long-channel devices this term must vanish). But the increase of $\partial^2 \psi / \partial z^2$ cannot follow the increase of V_{DS} endlessly; for higher values of V_{DS} this term is expected to become saturated. First, the longitudinal term $\partial^2 \psi / \partial z^2$ starts to dominate over radial term $\left(\frac{\partial^2 \psi}{\partial r^2} + \frac{1}{r} \frac{\partial \psi}{\partial r} \right)$ either for large values of V_{DS} or for

small values of channel length L . Second, so strong lateral electric field (much stronger than the radial one) begins to remove mobile charges from the silicon body and so creates the depleted region spreading from drain to source terminal. A described assumption can be written in the following manner [4]:

for small values of V_{DS}

$$\frac{\partial^2 \psi}{\partial z^2} = \frac{V_{DS}}{L^2} \quad (2a)$$

for extremely large values of V_{DS}

$$\frac{\partial^2 \psi}{\partial z^2} = \frac{qN_A}{\epsilon_{Si}} \quad (2b)$$

The next step followed the idea to meet the both of these two requirements, as well as to successfully express

this longitudinal term in the case of medium V_{DS} voltages. A good and prospective candidate with such performances is a simple expression:

$$\frac{\partial^2 \psi}{\partial z^2} = \frac{qN_A}{\epsilon_{Si}} \left[1 - \exp \left(- \frac{\epsilon_{Si}}{qN_A L^2} V_{DS} \right) \right] \quad (3)$$

The advantage of such assumption is recognized if the lateral term described by one-piece expression (3) is inserted into two-dimensional Poisson's equation (1):

$$\frac{\partial^2 \psi}{\partial r^2} + \frac{1}{r} \frac{\partial \psi}{\partial r} + \frac{q}{\epsilon_{Si}} N_A \left[1 - \exp \left(- \frac{\epsilon_{Si}}{qN_A L^2} V_{DS} \right) \right] = \frac{qN_A}{\epsilon_{Si}} + \frac{qn_i}{\epsilon_{Si}} \exp \frac{\psi - \psi_F}{\phi_t} \quad (4)$$

which is immediately reduced to its following form:

$$\frac{\partial^2 \psi}{\partial r^2} + \frac{1}{r} \frac{\partial \psi}{\partial r} = \frac{q}{\epsilon_{Si}} N_A \exp \left(- \frac{\epsilon_{Si}}{qN_A L^2} V_{DS} \right) + \frac{qn_i}{\epsilon_{Si}} \exp \frac{\psi - \psi_F}{\phi_t} \quad (5)$$

This way two-dimensional analysis of the problem has been reduced to one-dimensional case. Fortunately, the obtained equation (5) is exactly of the same form as the equation describing one-dimensional problem:

$$\frac{\partial^2 \psi}{\partial r^2} + \frac{1}{r} \frac{\partial \psi}{\partial r} = \frac{q}{\epsilon_{Si}} N_A + \frac{q}{\epsilon_{Si}} n_i \exp \frac{\psi - \psi_F}{\phi_t} \quad (6)$$

The only difference between equations (5) and (6) is the presence of drain-to-source voltage V_{DS} in equation (5) as a parameter. Effectively, the doping concentration N_A seems to be renormalized as follows [4]:

$$N_A \rightarrow N_A \exp(-\lambda V_{DS}), \quad \lambda = \frac{\epsilon_{Si}}{qN_A L^2} \quad (7)$$

i.e. it is reduced to significantly lower values. The solution of the equation (6) is well known in the literature; because of its significance it is cited here once again:

and

$$\psi(r, z) = \frac{qN_A R^2}{4\epsilon_{Si}} \left(\frac{r}{R} \right)^2 + V(z) - 2\phi_t \ln \left[\frac{R}{2} \sqrt{\frac{qn_i}{2\epsilon_{Si}\phi_t}} \frac{1 - (1-\alpha) \frac{r^2}{R^2}}{\sqrt{1-\alpha}} \right], \quad r \leq R$$

and

$$\psi(r, z) = C_1(z) \ln \frac{r}{R} + C_2(z), \quad R \leq r \leq R + t_{ox} \quad (8)$$

Parameter $\alpha \in (0,1)$ is credibly argued in the available literature and turns out to be crucial for the derivation of current-voltage characteristic. Following this way the solution to equation (5) can be written in a straightforward manner:

$$\psi(r, z) = \frac{qR^2}{4\epsilon_{si}} N_A \exp(-\lambda V_{DS}) \left(\frac{r}{R}\right)^2 + V(z) - 2\phi_t \ln \left[\frac{R}{2\sqrt{2\epsilon_{si}\phi_t}} \frac{1 - (1-\alpha)\left(\frac{r^2}{R^2}\right)}{\sqrt{1-\alpha}} \right], 0 \leq r \leq R, \quad (9a)$$

$$\psi(r, z) = C_1(z) \ln \frac{r}{R} + C_2(z), \quad R \leq r \leq R + t_{ox} \quad (9b)$$

The quasi-Fermi potential $V(z)$ introduced instead of Fermi potential ψ_F takes values $V(0)=0$ and $V(L)=V_{DS}$ at source and drain terminals, respectively and provides the potential dependence on the coordinate z . The solution (9a) and (9b) is completed with the usual set of boundary conditions describing the electrostatics without any charges at the interface:

$$\psi(R + t_{ox}, z) = V_g, \quad \psi(R^-, z) = \psi(R^+, z)$$

$$\epsilon_{si} \frac{d\psi}{dr} \Big|_{R^-, z} = \epsilon_{ox} \frac{d\psi}{dr} \Big|_{R^+, z} \quad (10)$$

The elimination of $C_1(z)$ and $C_2(z)$ from relation (9b) by means of relation (10) directly provides quasi-Fermi potential dependence on parameter α :

$$\begin{aligned} S \left[2\phi_t \frac{1-\alpha}{\alpha} + \frac{qR^2}{4\epsilon_{si}} N_A (2-\alpha) \exp(-\lambda V_{DS}) \right] = \\ = V_g - V(z) - \frac{qR^2}{4\epsilon_{si}} N_A \frac{3-\alpha}{2} \exp(-\lambda V_{DS}) + 2\phi_t \ln \left(\frac{R}{2\sqrt{1-\alpha}} \sqrt{\frac{qn_i}{2\epsilon_{si}\phi_t}} \right) \end{aligned} \quad (11)$$

with the following abbreviation:

$$S = 2 \frac{\epsilon_{si}}{\epsilon_{ox}} \ln \left(1 + \frac{t_{ox}}{R} \right) \quad (12)$$

Relation (11) is of crucial importance for the final aim of this paper, i.e. the construction of current-voltage characteristic.

3. Current-voltage characteristic

In the frame of drift-diffusion model the infinitesimal drain current through the infinitesimal symmetrical cross-section of cylindrical surrounding gate MOSFET becomes [5]:

$$dI_D = qn(r, z) \frac{dV}{dz} 2\pi r dr \quad (13)$$

Integrating relation (13) over the cross-section of the cylinder one immediately obtains [6]:

$$I_D = \mu_0 8\pi \epsilon_{si} \phi_t (1-\alpha) \frac{dV}{dz} f(\alpha) \quad (14)$$

where $f(\alpha)$ denotes [1]:

$$f(\alpha) = \frac{2}{R^2} \int_0^R \frac{\exp\left(\frac{qR^2}{4\epsilon_{si}\phi_t} \frac{r^2}{R^2} N_A \exp(-\lambda V_{DS})\right)}{\left[1 - (1-\alpha) \frac{r^2}{R^2}\right]^2} r dr \quad (15)$$

Relation (14) is now integrated over longitudinal coordinate z from source to drain terminal [6]:

$$I_D = \frac{\mu_0 8\pi \epsilon_{si} \phi_t}{L} \int_0^{V_{DS}} (1-\alpha) f(\alpha) dV = \frac{\mu_0 8\pi \epsilon_{si} \phi_t}{L} \int_{\alpha_s}^{\alpha_d} (1-\alpha) f(\alpha) \frac{dV}{d\alpha} d\alpha \quad (16)$$

The derivative $dV/d\alpha$ is simply calculated from relation (13):

$$\frac{dV}{d\alpha} = \phi_t \left[\frac{2S}{\alpha^2} + \frac{1}{1-\alpha} + \frac{2}{\alpha} + (2S+1) \frac{qR^2}{8\epsilon_{si}\phi_t} N_A \exp(-\lambda V_{DS}) \right] \quad (17)$$

while α_s, α_d denote the values of parameter α at the source and drain end, respectively. They are straight-forward obtained using relation (11) with described boundary conditions:

$$\begin{aligned} \frac{S}{\alpha_s} + \frac{1}{2} \ln(1-\alpha_s) - \ln \alpha_s - \left(S + \frac{1}{2} \right) \frac{qR^2}{2\epsilon_{si}\phi_t} N_A \alpha_s \exp(-\lambda V_{DS}) = \\ = \frac{V_g}{2\phi_t} - \frac{qR^2}{8\epsilon_{si}\phi_t} \left(2S + \frac{3}{2} \right) N_A \exp(-\lambda V_{DS}) + \ln \left(\frac{R}{2\sqrt{2\epsilon_{si}\phi_t}} \sqrt{\frac{qn_i}{2\epsilon_{si}\phi_t}} \right) \end{aligned} \quad (18a)$$

$$\begin{aligned} \frac{S}{\alpha_d} + \frac{1}{2} \ln(1-\alpha_d) - \ln \alpha_d - \left(S + \frac{1}{2} \right) \frac{qR^2}{2\epsilon_{si}\phi_t} N_A \alpha_d \exp(-\lambda V_{DS}) = \\ = \frac{V_g - V_{DS}}{2\phi_t} - \frac{qR^2}{8\epsilon_{si}\phi_t} \left(2S + \frac{3}{2} \right) N_A \exp(-\lambda V_{DS}) + \ln \left(\frac{R}{2\sqrt{2\epsilon_{si}\phi_t}} \sqrt{\frac{qn_i}{2\epsilon_{si}\phi_t}} \right) \end{aligned} \quad (18b)$$

For the values of geometric and technological parameters anticipated in this paper the evaluation of $f(\alpha)$ (15) can be considerably simplified. It is easily argued that the exponent in relation (15) can be expanded into series with only first and second terms retained. After tedious, but straight-forward transformations, relation (15) gets its final form:

$$f(\alpha) \approx \frac{1}{\alpha} + \frac{qN_A R^2}{4\epsilon_{si}\phi_t} \frac{1 + \alpha \ln \alpha - \alpha}{\alpha(1-\alpha)^2} \exp(-\lambda V_{DS}) \quad (19)$$

At the end of current-voltage characteristic construction procedure is useful to remind the reader that the mobility is set constant (μ_0) over the whole structure. Relations that complete the compact model deserve to be mentioned again: (16), (17), (18) and (19).

4. Numerical results and model verification

The consequences of the suggested procedure are tested for a specific set of geometric and technological parameters (Table 1).

Table 1. Geometrical and technological parameters used for model testing

$t_{ox}=1.5\text{nm}$	$\epsilon_{Si}=11.8 \cdot 8.85 \cdot 10^{-12}\text{F/m}$	$L=300\text{nm}$
$R=5\text{nm}$	$\epsilon_{ox}=3.9 \cdot 8.85 \cdot 10^{-12}\text{F/m}$	$L=40\text{nm}$
$N_A=10^{24}\text{m}^{-3}$	$V_G=1\text{V}$	$L=30\text{nm}$
	$\mu_0=0.2\text{m}^2/(\text{V}\cdot\text{s})$	$L=20\text{nm}$
		$L \rightarrow 0$

The algebraic equations (18a) and (18b) are easily solved using any of available numerical tools. Relations (17) and (19) are simply inserted into expression (16), which is then integrated without any problems. Although the numerical treatment is necessary and the model cannot be recognized as analytical, it is still simple enough to be incorporated into more complex electronic circuits and convenient enough for CAD (computer-aided-design).

For the sake of having better insight into obtained results the calculated current-voltage characteristic has been shown in Figs. 2 and 3. Fig. 2 brings drain current in dimensionless form, i.e. the real drain current is divided by a constant term [7, 8]:

$$I_D^* = \frac{I_D}{\mu_0 \frac{8\pi\epsilon_{Si}\phi_t^2}{L}} \quad (20)$$

for various values of channel length as a parameter. The intention of introducing this way normalized drain current was to underline the consequences of the calculating procedure suggested in this paper. Several interesting and intriguing conclusions emerge.

First, the normalized drain current globally decreases if the channel length L scales down. For hypothetically small values of L ($L \rightarrow 0$) the influence of doping concentration is lost and our result tends to undoped sample result (e) which lies far below the others (a, b, c, d).

Second, for ultra high values of drain-to-source voltage V_{DS} , the normalized doping concentration described by relation (7) is reduced to zero, causing this way the same effect as $L \rightarrow 0$. The consequence is that all the graphs for different L (a, b, c, d, e) meet together as horizontal lines for high values of V_{DS} . Therefore graphs (a, b, c, d) show the feature of negative differential

resistance. This might be surprising since even the announcement of negative differential resistance has not been observed in the case of planar devices. So, if true, it can be explained as a direct consequence of cylindrical geometry of investigated devices. It is also fair to say that the described unique asymptotic behavior of graphs (a, b, c, d) happens for such high values of drain-to-source voltage V_{DS} , hence playing no significant role for practical purpose.

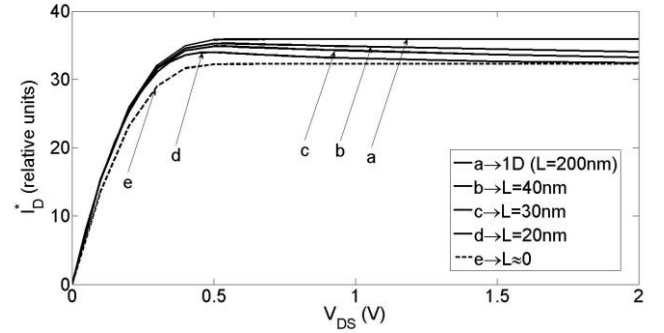


Fig. 2. Normalized drain current I_D^* (in relative units) versus drain-to-source voltage V_{DS} for various channel length as a parameter

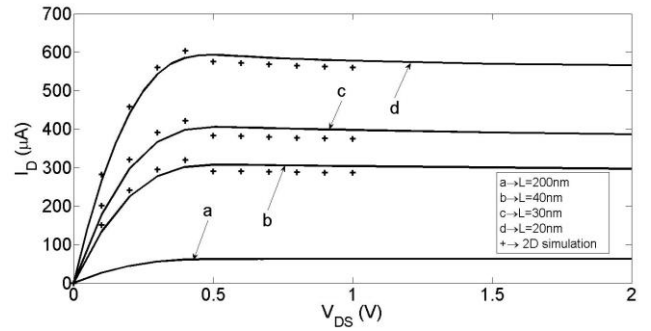


Fig. 3. Drain current I_D according to relation (20) versus drain-to-source voltage V_{DS} for various values of channel length

Fig. 3 brings the real drain current I_D versus drain-to-source voltage V_{DS} , either calculated according to the suggested model or the results obtained using conventional simulation tools (ATLAS...) [9]. The situation seems to be quite different from one described in Fig. 2; Owing to L^{-2} dependence of relation (20) the real drain current is increased as the channel length scales down. The slightly announced negative differential resistance region is still present for $V_{DS} > 0.5\text{V}$, while the agreement with 2D simulation results is satisfactory.

5. Conclusion

In this paper the original procedure for approximate analytical solving of two-dimensional Poisson's equation has been carried out. Based on this solution, a new model of current-voltage characteristic for short-channel nanowire MOSFETs has been proposed. This model is entirely analogous to the (one-dimensional) long-channel

nanowire MOSFETs model and can be recognized as its natural extension to the two-dimensional case. The developed procedure is applicable even in the case when the mobile charge concentration is not negligible, i.e. in the above threshold regime and is free of fitting parameters. The model has been verified by comparison with 2D simulations.

Acknowledgements

This work was financially supported by the Ministry of Science and Technological Development, Republic of Serbia; Project III 45003 and Project 43011.

References

- [1] S. M. Ostojić, R. M. Šašić, P. M. Lukić, I. Abood, *Phys. Scr.* **89**(11), 1 (2014).
- [2] R. Šašić, R. Ramović, V. Herrmann, *Phys. Stat. Sol.* **165a**, 445 (1998).
- [3] B. Yu, Y. Yuan, J. Song, Y. Taur, *IEEE Trans. Electron Devices* **56**(10), 2357 (2009).
- [4] X. Jin, X. Lin, Jung-H. Lee, Jong-H. Lee, *Phys. Scr.* **89**, 015804 (2014).
- [5] J-P. Colinge, D. Lederer, A. Afzalian, R. Yan, C-W. Lee, N. D. Akhavan, D. Xiong, *Japan J. Appl. Phys.* **48**, 034502 (2009).
- [6] D. Jimenez, B. Iniguez, J. Sune, L. F. Marsal, J. Pallares, J. Roig, D. Flores, *IEEE Electron Device Lett.* **25**, 571 (2004).
- [7] A. A. Alkoash, R. M. Šašić, P. M. Lukić, S. M. Ostojić, *J. Comput. Theor. Nanosci.* **8**, 47 (2011).
- [8] B. Yu, W.-Y. Lu, H. Lu, Y. Taur, *IEEE Trans. Electron Devices* **54**, 492 (2007).
- [9] X. Jin, X. Liu, M. Wu, R. Chuai, J-H. Lee, J-H. Lee, *Semicond. Sci. Technol.* **28**, 129901 (2013).

*Corresponding author: stankos@afrodita.rcub.bg.ac.rs